Proceedings of the 14th IEEE
International Conference on Nanotechnology
Toronto, Canada, August 18-21, 2014

Epitaxial growth of NaCl on Fe (100) and characterization of Fe/NaCl/Fe magnetic tunnel junctions

Yuan-Tao Ji, Qiang Li, Yong-Chao Tang, Lin Li and Guo-Xing Miao

***Abstract* — Growth of NaCl and Fe/NaCl/Fe Magnetic tunneling junctions on Si (100) has been achieved by using a high vacuum electron-beam deposition system. Epitaxial tunnel junctions turn out to be prone to pinholes as well as electrode oxidation. Instead, the best tunneling magnetoresistance we have achieved in this system is on polycrystalline tunnel barriers with thin Mg insertion, and reaching 22.3% at room temperature.**

Index Terms – Nanodevices, Spintronics, magnetic tunnel junctions, Tunnel magnetoresistance, NaCl.

I. Introduction

The tunneling magnetoresistance (TMR) phenomenon in magnetic tunnel junctions (MTJs) has led to the revolution of data storage and magnetic sensing devices in the past two decades. Its most profitable industrial applications include nonvolatile data storage in hard drive and magnetic random access memory (MRAM) [1, 2].

Butler *et al.* [3] have predicted that the TMR of epitaxial Fe/MgO/Fe (001) junctions should be higher than 1000% if the Bloch state symmetry of the tunnel electrons is also conserved during the tunneling process [4]. Based on similar models, Vlaic *et al.* [5] have calculated that TMR of epitaxial Fe/NaCl/Fe (001) should also be higher than 1000%, and Tao *et al.* [6] theoretically predicted similar performance in FePt/NaCl/FePt (001) tunnel junctions. Since the crystal structure and the band structure of NaCl are quite similar to those of MgO [7 - 9], and can be grown epitaxially on Fe [4], it is another promising barrier material for establishing coherent tunneling in MTJs [10 - 15]. In addition, because NaCl contains only light elements, just like the most popular barrier materials Al_2O_3 and MgO [16], it is not much influenced with spin scattering inside the barrier and offers better spin transport efficiency [17 - 19]. In the present work, we fabricated Fe/NaCl/Fe MTJs under various growth conditions. The TMR and the current–voltage characteristics are investigated.

II. Experimental and Results

The magnetic tunnel junctions consist of two Fe layer as top and bottom electrodes with a NaCl layer in the middle as the tunnel barrier. Samples were deposited in a high vacuum e-beam and thermal evaporation system. The system base pressure is better than 1E-8 Torr. Fe, MgO, NaCl are deposited by electron beam evaporation, while Mg is deposited by thermal evaporation. Because of the water solubility of NaCl, conventional lithography process is not possible in junction fabrications. Instead, we have developed an *in situ* shadow-masking technique to create tunnel junctions without breaking vacuum.

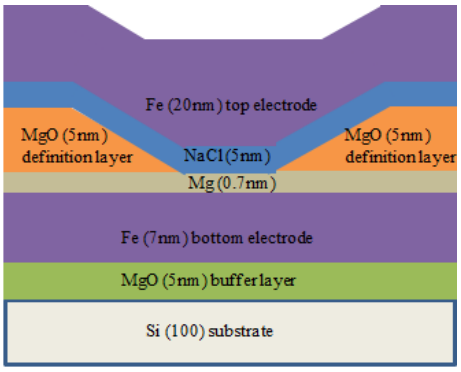

Fig. 1 schematic structure of Fe/NaCl/Fe Magnetic Tunnel Junctions (MJTs)

The chamber pressure was kept in the 10^-8 Torr range during the active layers' depositions, except the step when the junction area was defined by MgO definition layers. The system pressure goes into the 10^-7 Torr range and some oxidation on the bottom electrode may be expected. The sample preparation process is as follows. A 5 nm MgO (100) buffer layer was grown on HF etched Si (100) wafer at 300°C. After the sample cools down to room temperature, a 7 nm Fe layer was deposited as the bottom electrode. XRD confirmed that the bottom electrode is epitaxial throughout all the samples studied in this work. In our best tunnel junctions achieved, several atomic layers of Mg were deposited to protect the bottom electrode from being oxidized. After formation of the bottom electrode, the junction definition is formed with 10nm MgO evaporated through micro shadow masks, leaving the active junction region of 30×30 μm^2 uncovered in order to form junctions with the subsequent top electrode. The sample was then heated to 150°C to deposit several different thicknesses of

978-1-4799-5622-7/$31.00 ©2014 IEEE

NaCl barrier layers, ranging from 2 nm to 5 nm. Finally, 20 nm Fe was deposited also at 150ºC as the top electrode followed with a 20 nm Ti protection layer. The growth rate was maintained at 0.1 Å/s for all of the layers. DC transport measurement was performed with four terminal method in sweeping magnetic fields, and for 77K measurement, liquid nitrogen was directly introduced to the sample space and submerged the samples.

III. Results and Discussions

A. *Epitaxial Growth of NaCl on Fe*

XRD and its pole figure mapping confirmed the epitaxy of the MgO buffer layer on Si and the bottom Fe electrode. A few different configurations were used for the tunnel barrier and top electrode. When NaCl and top Fe were directly deposited onto bottom Fe at 150ºC, the stack is fully epitaxial. Fig. 2 showed the θ-2θ scan of such a stack with 3 nm NaCl barrier, and the MgO, Fe, and NaCl are all in their (100) orientation. We also performed off-axis ψ scan on the Fe (110) reflections to verify the top electrode is still epitaxial. As expected from prior knowledge, the Fe layers are 45° rotated in-plane relative to the Si substrate. To determine the orientation of NaCl, we deposited a control sample with epitaxial Fe bottom electrode followed by a 30 nm NaCl layer protected with Al_2O_3 capping. The NaCl (111) reflection showed clearly four fold symmetry under ψ rotation, and NaCl lattice is determined to be also 45° rotated relative to Si, therefore aligned straight with Fe lattices. The bulk lattice parameters of NaCl and Fe are 5.640 Å and 2.867 Å, respectively, with only a small lattice mismatch of -1.6% and a good epitaxy correlation expected between them. On the other hand, the top Fe electrode (110) reflection showed a peak broadening of about 5° with ψ rotation, indicating that significant texturing is present despite the overall epitaxy in the samples.

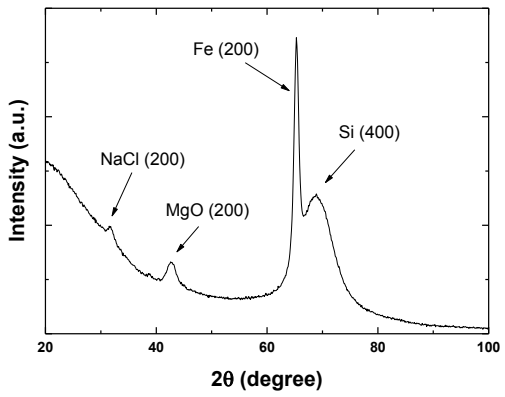

Fig. 2 XRD θ-2θ scan of a magnetic tunnel junction without Mg insertion. The layers' thicknesses are (in nm): (100)-Si substrate / 5 MgO / 7 Fe / 3 NaCl / 20 Fe. To avoid the intense Si (400) diffraction and its satellite peaks, the ω angle was offset by 2.5° in the scan.

B. *Characterization of Fe/NaCl/Fe Magnetic Tunnel Junctions with Mg Insertion*

Though being nicely epitaxial, the samples without Mg insertion were mostly shorted due to the presence of intense pinholes through the NaCl tunnel barrier, which is attributed to the island-growth of NaCl directly on Fe. Instead, the best TMR we have obtained was on samples with ultrathin Mg insertion, which is subsequently oxidized into MgO in the step of junction definition, when the chamber pressure rise to above 10^{-7} torr due to oxygen released from decomposed MgO. This ultrathin Mg (which is converted into MgO soon after) is introduced to modify the surface chemistry in order to promote layer-by-layer growth, and also to function as an oxidation barrier for the bottom electrode.

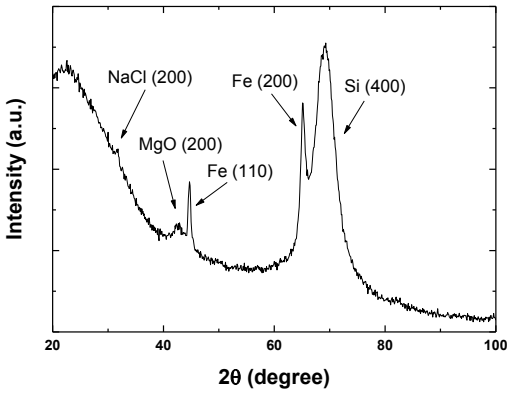

Fig. 3 XRD θ-2θ scan of a magnetic tunnel junction with Mg insertion. The layers' thicknesses are (in nm): (100)-Si substrate / 5 MgO / 7 Fe / 0.7 Mg / 3 NaCl / 20 Fe. To avoid the intense Si (400) diffraction and its satellite peaks, the ω angle was offset by 2.5° in the scan.

This approach is similar to the concept used by Tekiel *et al* in using FeO as the promotion for layer-by-layer NaCl growth [20], where they clearly identified the desired growth mode with *in situ* scanning tunneling microscopy (STM). With the Mg insertion, we found that the subsequent growth of NaCl and the top Fe electrode are both polycrystalline because Mg interrupted the potential epitaxy correlations with the bottom electrode. On the other hand, due to the polycrystalline nature of the growth, we can to a large extent avoid the pinhole formation in the barriers. Fig.4 shows the typical magnetoresistance curve of such a tunnel junction, TMR ratio reaching 22.3% at room temperature and 37.8% at liquid nitrogen temperature. The devices follow the standard TMR behavior, showing a nonlinear I-V response curve (Fig.5), and a gradually decreasing TMR with increased applied bias voltages (Fig.6). The junction's conductance and magnetoresistance are very symmetric with respect to the applied bias voltage, indicating that the thin Mg insertion did not modify much the barrier's energy profile. TMR decreases from its peak value of 22.3% to 11.8% at 0.3 V (the upper bound of our measurement), indicating that the TMR V_{half} is higher than 0.3 V and is suitable for room temperature applications.

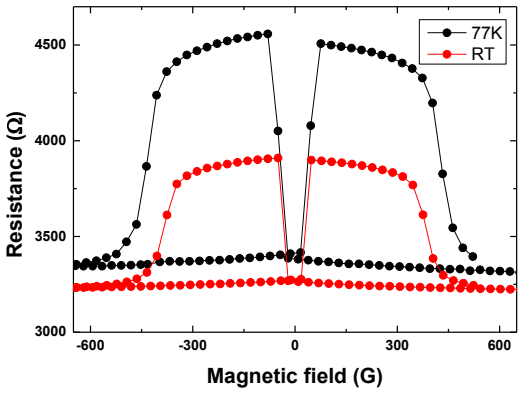

Fig. 4 Tunneling magnetoresistance response measured at room temperature (red) and liquid nitrogen temperature (black).

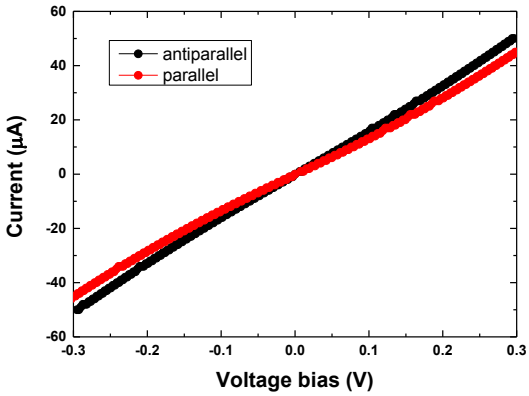

Fig. 5 The I-V characteristics of the tunnel junction in its spin parallel and antiparallel configurations at room temperature.

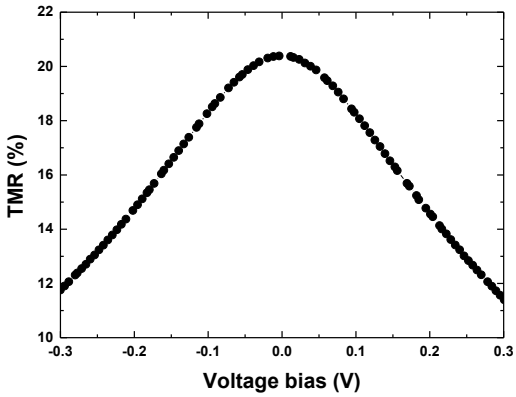

Fig. 6 TMR ratio vs bias voltage at room temperature.

Currently, the magnetoresistance is not as high as what we would expect from a perfect, epitaxial Fe/NaCl/Fe magnetic tunnel junction. The major challenge is to eliminate the pinhole formations in the NaCl barrier which is a direct consequence of NaCl's island growth mode. Passivating the Fe surface with oxides helps promoting more uniform barrier coverage. However, the formation of FeO on the tunnel junction barrier turned out significantly reducing the obtained TMR in our devices. We therefore used ultrathin Mg insertion layer below the tunnel barrier to prevent electrode oxidation while still forms a MgO-like surface before the NaCl growth. As a trade-off, the epitaxy correlation was broken starting from this interface leading to the less-than-expected TMR performance. In principle, NaCl has a lattice constant reasonably close to MgO (when 45° rotated) with a mismatch of -5.3%, and we should be able to establish epitaxy even in the presence of the Mg (MgO) insertion layer. In practice, it turned out that although 150°C is high enough for epitaxial growth of NaCl on Fe (-1.6% mismatch), it is not sufficient to get epitaxial NaCl on MgO. Further raising NaCl growth temperature once again led to pinholes in the junctions, and our optimized junctions reported here were all deposited at 150°C as a compromise.

IV. Conclusion

We have studied Fe/NaCl/Fe based magnetic tunnel junctions and the system was optimized with the balancing between epitaxy, pinhole formation, and electrode oxidation. We obtained sizeable TMR over 22% at room temperature in this system.

Acknowledgment

This work is supported by NSERC Discovery grant.

References

[1] Bader, S. D., and S. S. P. Parking. "Spintronics." Annul. Rev. Condens. Matter Phys. 1.1 (2010): 71-88.
[2] Miao, Guo-Xing, Markus Münzenberg, and Jagadeesh S. Moodera. "Tunneling path toward spintronics." Reports on Progress in Physics 74.3 (2011): 036501.
[3] Butler, W. H., et al. "Spin-dependent tunneling conductance of Fe| MgO| Fe sandwiches." Physical Review B 63.5 (2001): 054416.
[4] Nakazumi M, Yoshioka D, Yanagihara H, et al. Fabrication of magnetic tunneling junctions with NaCl barriers[J]. Japanese Journal of Applied Physics, 2007, 46(10R): 6618.
[5] Vlaic P. Calculated magnetic and transport properties of Fe/Nacl/Fe (001) magnetic tunnel junction [J]. Journal of Magnetism and Magnetic Materials, 2010, 322(9): 1438-1442.
[6] Tao, L. L., et al. "Tunneling magnetoresistance of FePt/NaCl/FePt (001)." EPL (Europhysics Letters) 105.5 (2014): 58003.
[7] D. M. Roessler and W. C. Walker: Phys. Rev. 166 (1968) 599.
[8] N. O. Lipari and A. B. Kunz: Phys. Rev. B 3 (1971) 491.
[9] Miao, G. X., et al. "Epitaxial growth of MgO and Fe⁄ MgO⁄ Fe magnetic tunnel junctions on (100)-Si by molecular beam epitaxy." Applied Physics Letters 93.14 (2008): 142511.

[10] Miao, G. X., et al. "Disturbance of tunneling coherence by oxygen vacancy in epitaxial Fe/MgO/Fe magnetic tunnel junctions." Physical review letters 100.24 (2008): 246803.
[11] Meservey, Robert, and P. M. Tedrow. "Spin-polarized electron tunneling." Physics Reports 238.4 (1994): 173-243.
[12] Mavropoulos, Ph, N. Papanikolaou, and P. H. Dederichs. "Complex band structure and tunneling through ferromagnet/insulator/ferromagnet junctions." Physical review letters 85.5 (2000): 1088.
[13] Tsymbal, E. Yu, and D. G. Pettifor. "Modelling of spin-polarized electron tunnelling from 3d ferromagnets." Journal of Physics: Condensed Matter 9.30 (1997): L411.
[14] Mathon, J., and A. Umerski. "Theory of tunneling magnetoresistance of an epitaxial Fe/MgO/Fe (001) junction." Physical Review B 63.22 (2001): 220403.
[15] Moodera, Jagadeesh S., and George Mathon. "Spin polarized tunneling in ferromagnetic junctions." Journal of magnetism and magnetic materials 200.1 (1999): 248-273.
[16] Moodera, Jagadeesh Subbaiah, et al. "Large magnetoresistance at room temperature in ferromagnetic thin film tunnel junctions." Physical Review Letters 74.16 (1995): 3273.
[17] Mazin, I. I. "How to define and calculate the degree of spin polarization in ferromagnets." Physical Review Letters 83.7 (1999): 1427.
[18] Viret, M., et al. "Spin scattering in ferromagnetic thin films." Physical Review B 53.13 (1996): 8464.
[19] Jansen, R., and J. S. Moodera. "Magnetoresistance in doped magnetic tunnel junctions: Effect of spin scattering and impurity-assisted transport." Physical Review B 61.13 (2000): 9047.
[20] A. Tekiel, J. Topple, Y. Miyahara, P. Grutter, Nanotechnology 23 (2012) 505602.